SIMULATING IONOSPHERE SCINTILLATION EFFECTS. POTENTIAL APPLICATIONS FOR FUTURE EARTH OBSERVATION MISSIONS.

Laura Fernández

GMV Aerospace and Defence, Isaac Newton 11, P.T.M. Tres Cantos. E-28760, Madrid, Spain

Abstract

In real soundings of the Earth's atmosphere, it has been found that the phase and amplitude of the signal received undergo strong oscillations at altitudes above the neutral atmosphere and below the E-layer of the ionosphere. This ionospheric scintillation effect is a consequence of multipath propagation resulting from inhomogeneities in the refractivity field of the ionosphere.

Ionospheric scintillations can become a problem when processing radio occultation measurements to retrieve geophysical parameters (e.g. temperature and pressure), particularly when trying to achieve high accuracies in the retrieved profiles. Therefore, the impact of ionospheric scintillation effects needs to be carefully valuated.

Current ionospheric scintillation models are calibrated empirically. Thus, their applicability to different radio frequencies, scintillation conditions and geometric configurations is not straightforward. We have developed a method to simulate ionospheric scintillation effects on radio occultation measurements. The flexibility of the model presented allows testing many different configurations. The model can be useful in the remote sensing field for assessing radiowave propagation effects through a strongly perturbed ionosphere. It can also be used to evaluate the performance of scintillation mitigation techniques, in the context of satellite based navigation systems.

INTRODUCTION

Ionospheric scintillation of a radio signal is a relatively rapid fluctuation of the amplitude, phase and Faraday rotation angle of the signal around mean levels which are either constant or changing much more slowly than the scintillations themselves. Ionospheric scintillations are caused by irregularities of the ionospheric electron density encountered along the signal propagation path.

The performance of Radio Occultation (RO), navigation and communication systems can be compromised in the presence of ionospheric scintillations. In the Global Navigation Satellite Systems (GNSS) field, ionospheric scintillations may induce loss of lock, cycle slips or excessive phase noise on ranging signals broadcast by the GNSS satellites, making them totally useless for accurate integrity determination and reducing GNSS availability significantly (Fernández et al, 2008). In the context of RO phenomena, as the RO signal crosses the lower ionosphere E-layer, it may encounter sharp vertical electron density gradients and get disturbed, resulting in strong amplitude and phase scintillations in RO measurements at 80–100Km (Sokolovskiy et al, 2002). Sometimes these ionospheric perturbations are so strong that they result in multipath propagation (Gorbunov et al, 2002).

There is a need to assess the amplitude of the errors caused by propagation through these ionospheric perturbations. The situation is particularly demanding for future Earth Observation missions, which aim at reaching an increased accuracy in the observations.

Current ionospheric scintillations models (Béniguel 2002 and Secan et al 1995) are empirically calibrated using in-situ measurements from different sources. Therefore, the applicability of such

models to different radio frequencies, scintillations conditions and geometric configurations is not straightforward (Forte et al, 2005). Moreover, when trying to obtain strong scintillation conditions, the models do not seem to provide realistic results, since they have been calibrated with scintillation data obtained in significantly less aggressive conditions (Hernández et al, 2006). Lastly, there is a lack of atmospheric measurements with sufficient spatial resolution to match the small length scale of the ionospheric inhomogeneities.

This paper presents the simulation results of an analytical propagation model, able to simulate the effects of ionospheric scintillations on RO measurements. The main advantage of an analytical model over statistical or empirical approaches is that it allows exploring different configurations. Scintillations events are highly influenced by several parameters such as the strength, scale and location of the ionospheric irregularities, the signal frequency or the transmitter and receiver relative geometries. We will assess the impact of some of these parameters on the characteristics of the scintillations events, considering different configurations representative of what can realistically be observed.

The paper is organized as follows. The first section briefly outlines the basics of the RO phenomenon, followed by a description of how RO measurements are affected by ionospheric scintillations. The method employed in the simulations is described in the paper's next section, emphazising the atmosphere and propagation aspects. Then, the simulation studies are presented, followed by discussions on the results obtained. A final section presents our conclusions.

IONOSPHERIC SCINTILLATIONS IN RADIO OCCULTATION PHENOMENA

Radio Occultation Phenomenon

The RO phenomenon is illustrated in Figure 1. A radio signal from an emitting spacecraft (GNSS satellite) passes through the Earth's atmosphere before arriving at the receiver, which is placed in a Low Earth Orbit (LEO) satellite. The word "occultation" is used to refer to the fact that the position of both spacecrafts with respect to the Earth is such that, from the perspective of the receiver, the Earth is eclipsing the emitter. Thus, from the perspective of the receiver, the emitter is seen to be either rising or setting with respect to the limb of the occulting Earth. These two cases correspond to the so-called rising and setting occultations, respectively.

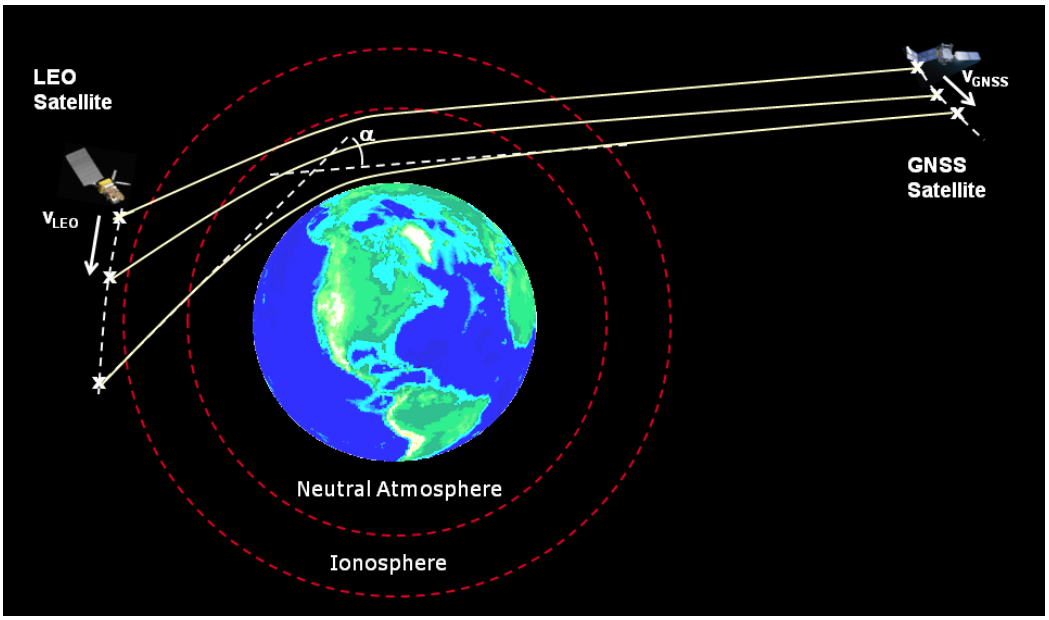

Figure 1: **Illustration of the RO phenomenon**

As the radio wave from the GNSS emitting satellite passes through the atmosphere, it is altered by the refracting medium. Specifically, the signal is bent towards the Earth (in a certain angle called the bending angle, α in Figure 1) and delayed in its arrival at the receiver. The ionosphere, which is traversed twice in the propagation (Figure 1), causes an extra delay (ionospheric delay) on the arrival of the signal at the receiver, apart from the one caused by the neutral atmosphere. Due to the dispersive nature of the ionosphere plasma, this delay is dependent on the signal frequency.

The RO measurements (i.e. the phase and amplitude of the wave at the receiver) are consequently altered relative to the values that would hold without the intervening medium or the occulting planet. As time evolves, profiles of the phase and amplitude variation at the receiver are generated and recorded by the receiver. These profiles provide information about the refractive properties of the intervening medium.

Ionospheric scintillations

The ionosphere is a region of ionized gas or plasma that extends from roughly 50 Km to a not very well defined upper limit of about 500 Km to 2000 Km above the Earth's surface. It contains free electrons that affect electromagnetic wave propagation. Ionization is produced by solar radiation, and therefore, the density of electrons in the ionosphere depends on altitude over the Earth (i.e. proximity to the Sun), solar activity and whether it is daytime or night time.

The ionosphere consists of several layers or regions of varying ion density. By increasing altitude and peak electron densities, these layers are known as the D, E, and F layers. The layers are not sharply defined since the transition from one to the other is generally gradual with no very pronounced minimum in electron density in between. The D-layer extends from approximately 50 to 90 Km, with very low electron concentration, and the maximum electron density occurring between 75 and 80 Km. The E-layer extends from about 90 to 140 Km, with the peak electron concentration occurring between about 100 and 110 Km. The F-layer has the highest electron densities of the ionosphere. The peak electron density is in the 200 to 400 Km height range.

Signals with frequencies above the ionospheric penetration frequency and up to about 10 GHz, when propagated through the ionosphere, are modified by the large- and small-scale variations of electron density encountered. The effect of these electron density irregularities on a propagating signal is called ionospheric scintillation and consists in a relatively rapid fluctuation of the amplitude, phase, polarization, and angle of arrival of the signal.

Although predominantly caused by irregularities in the F-layer, scintillations can also be produced by the E-layer irregularities. Within this group, we are interested in a particular kind of scintillation produced by the so-called sporadic E-layers (E_s). These areas belong to the lower ionospheric E-layer (between 90 and 120 Km) and present intense ionisation with electron densities well above 10^{12} electrons/m^3 (Ippolito, 1999). The very small height scale associated with the E_s makes the vertical electron density gradient largest there, which causes strong scintillation.

E_s irregularities are a problem for RO measurements, which are used to retrieve atmospheric profiles from the Earth's surface up to 90-120 Km. When propagated through the E_s, the RO signal is disturbed by the electron density spatial fluctuations encountered and present strong amplitude and phase fluctuations when it arrives at the LEO satellite.

The usual measure of the strength of amplitude scintillation is the S_4 index, defined as the normalized standard deviation of the signal intensity:

$$S_4 = \sqrt{\left(\frac{< A^4 >}{\left(< A^2 >\right)^2} - 1 \right)} \qquad (1)$$

Where *'A'* is the amplitude of the signal at the receiver and *'<>'* denotes averaging. Three categories can be established to classify the level of scintillation, based on S_4 index values: low activity ($S_4 < 0.3$), moderate activity ($0.3 < S_4 < 0.6$) and strong activity ($S_4 > 0.6$), see (Béniguel, 2000).

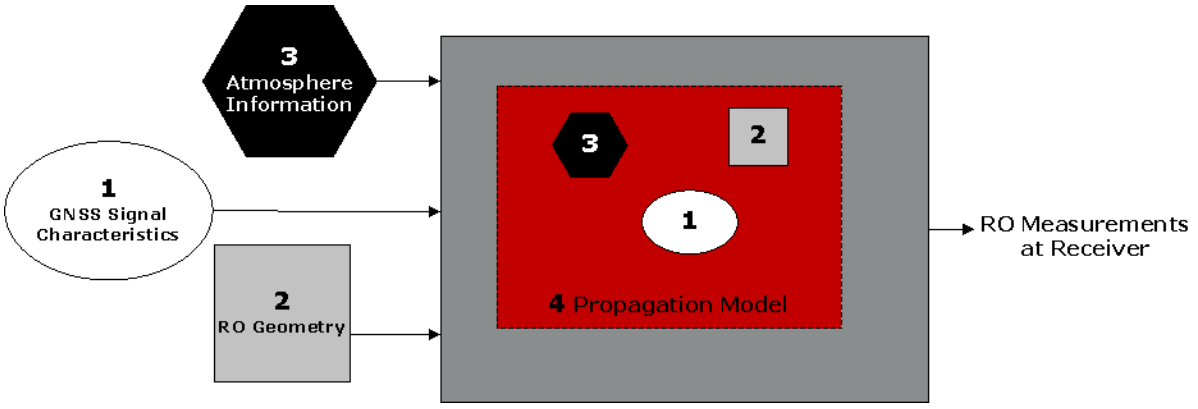

Figure 2: **High-level diagram of the RO simulator**

METHOD

As shown in Figure 2, four main aspects are accounted for in the simulation of RO measurements (particular emphasis is placed on the third and fourth aspects, which will be treated specifically in separate sections):

1. The GNSS Signals Model, i.e., the main characteristics of the GNSS signal that is being propagated. For the sake of computational efficiency in the propagation, we propagate GNSS signals without code modulation and only consider single monochromatic waves of configurable frequency.
2. The RO Geometry, i.e., the positions and velocities of the GNSS and LEO satellites with respect to the Earth during the RO phenomenon. This information is necessary in the simulation in order to determine the area in which propagation takes place and the source and destination of the GNSS signal. We consider satellite trajectories representative of real Global Positioning System (GPS) and LEO geometries.
3. The Atmospheric Model, i.e., the way in which the medium traversed by the signal (the Earth's Atmosphere) is represented.
4. The Propagation Model, i.e., the electromagnetic algorithms for the simulation of the GNSS signal propagation through the atmosphere, given the RO geometries of both satellites.

Atmospheric Model

We modeled a spherically symmetric analytical atmosphere, represented by the refractivity. For propagation of microwave frequencies in the Earth's atmosphere, the refractivity contains four different contributions. In order of importance, these contributions are: dry atmosphere (dry term), water vapour (wet term), free electrons in the ionosphere (ionospheric term) and liquid water (scattering term). This last term is small compared with the others and can therefore be neglected. The refractivity '*N*' is therefore given as function of height, *h*, through the following equation:

$$N(h) = (n-1)\cdot 10^6 = \underbrace{N_d \cdot e^{-(h/H_d)}}_{Dry\ Term} + \underbrace{N_w \cdot e^{-(h/H_w)}}_{Wet\ Term} \underbrace{- 4.03 \cdot 10^7 \frac{n_e(h)}{f^2}}_{Ionospheric\ Term} \quad (2)$$

The dry and wet terms in equation (2) are modelled as exponential functions of altitude, with different scale heights (H_d and H_w) and surface refractivities (N_d and N_w). The first-order ionosphere contribution to refractivity in equation (2) depends on the electron density, n_e, and the frequency of the signal, *f*. In the above equation, the refractive index is represented by '*n*'.

In the current context, the Earth's atmosphere is considered to be divided in two main regions: the neutral atmosphere (comprised by troposphere, stratosphere and mesosphere) and the ionosphere (Figure 1). Then, the dry and wet terms in equation (2) correspond to the neutral atmosphere region whereas the ionospheric term corresponds to the ionosphere region.

The electron density profile inside the medium is modeled by the summation of two terms:

$$n_e(h) = \underbrace{n_{eF}\,Chap\left(\frac{h-\xi_F}{H_F}\right) + n_{eE}\,Chap\left(\frac{h-\xi_E}{H_E}\right)}_{Background\ \ Ionosphere\ \ (Double\ Chapman\ \ Model)} + \underbrace{B\cdot e^{-(h-BH)^2/BW}}_{Fluctuation} \tag{3}$$

The first term in the above equation represents a background electron density function, given by the Double Chapman Ionospheric Model. Double Chapman formulation considers the existence of two layers in the ionosphere: the E-layer (located around 100 Km) and the F-layer (around 300 Km). We do not consider the D-layer because it tends to have little effect on the frequencies studied. *Chap(z)* in equation (3) is the Chapman function defined as:

$$Chap(z) = \exp(0.5(1 - z - \exp(-z))) \tag{4}$$

The second term in equation (3) represents a Gaussian-shaped fluctuation, with configurable altitude (*BH*), aperture (*BW*) and size (*B*). This fluctuation is used to introduce the vertical electron density gradients necessary for the simulation of ionospheric scintillation effects. The degree of scintillation can be easily adjusted through *BW* and *B* parameters.

Propagation Model

We numerically simulated the propagation of the GNSS signal using different solutions of the 2-D Helmholtz wave equation. The signal must be propagated as a wave to account for the multipath caused by the presence of electron density gradients. Depending on the medium traversed (vacuum or atmosphere, Figure 3), a different solution of Helmholtz equation is used.

For the signal propagation in the atmosphere, the Multiple Phase Screens (MPS) method is applied (Martin, 1993). This is a commonly used method that physically consists in dividing the continuous atmosphere into parallel slabs of length Δx, nearly orthogonal to the propagation direction ('*x*' axis in Figure 3). The field is propagated through the consecutive slabs using split-step methods applied to the parabolic equation (PE) derived from Helmholtz equation. The result of this MPS calculation is the field along the slab closest to the LEO satellite. The area to which the field propagation calculations are confined (indicated in red colour in Figure 3) is located by means of geometrical considerations.

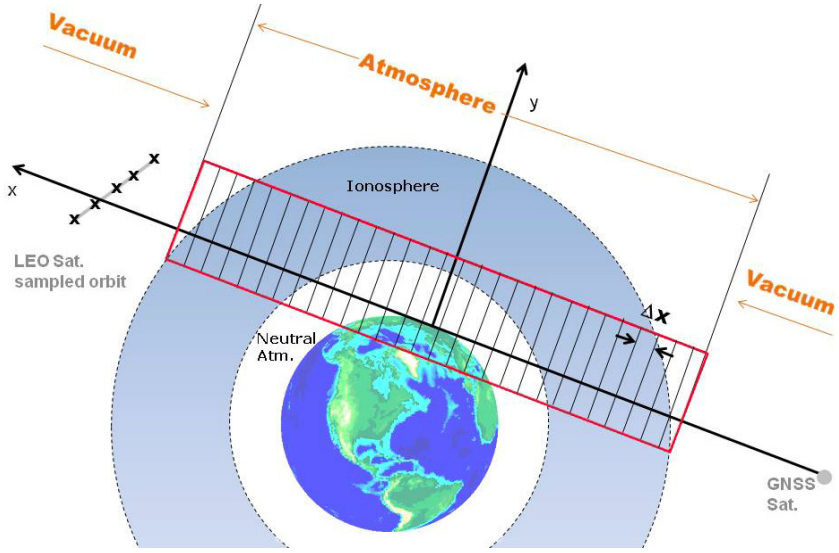

Figure 3: **Schematic view of the RO geometry**

SIMULATION RESULTS

We have simulated the ionospheric scintillation effect using the MPS technique described above for a GPS L1 signal (1575.42 MHz). The emitter and receiver are a GPS and LEO satellite placed approximately at an altitude of 20.000 Km and 800 Km, respectively. During the RO phenomenon, the satellites movement results in a normal speed setting occultation characterised by an elapsed time between 70 Km and 30 Km equal to 14 sec., and a Ray Tangent Height (RTH) immersion rate at 30 Km equal to 2.5 Km/sec. The RTH is defined as the closest distance between the bended ray and the Earth's ellipsoid.

For the neutral atmosphere, we considered dry and wet characteristic refractivities: N_d = 300 N units, H_d = 7.9 Km, N_w = 100 N-units and H_w = 2.5 Km. For the background ionosphere (represented in the left plot of Figure 4), the values for the double Chapman ionosphere model parameters (equation (3)) used in the simulations are provided in Table 1. These values correspond to daytime solar maximum conditions.

Symbol	Description	Value
n_{eF}	Maximum electron density of F-layer	3 10^{12} electrons/m^3
ξ_F	F-peak altitude	300 Km
H_F	F-layer scale height	50 Km
n_{eE}	Maximum electron density of E-layer	2 10^{11} electrons/m^3
ξ_E	E-peak altitude	105 Km
H_E	E-layer scale height	10 Km

Table 1: **Parameters of the Ionospheric double Chapman model. Values provided for daytime solar maximum conditions**

For the simulation of the scintillation effect ('*Fluctuation*' term in equation (3)), different perturbations in the electron density profile are superimposed at 80 Km (*BH*) to the background profile. The aperture of the perturbations is *BW*= 0.5 Km^2 and they have three different sizes, corresponding to different fluctuation levels: no fluctuation (*B* = 0 electrons/m^3), moderate fluctuation (*B* = 10^{11} electrons/m^3) and strong fluctuation (*B* = 5 10^{11} electrons/m^3). These perturbations are shown in the right plot of Figure 4.

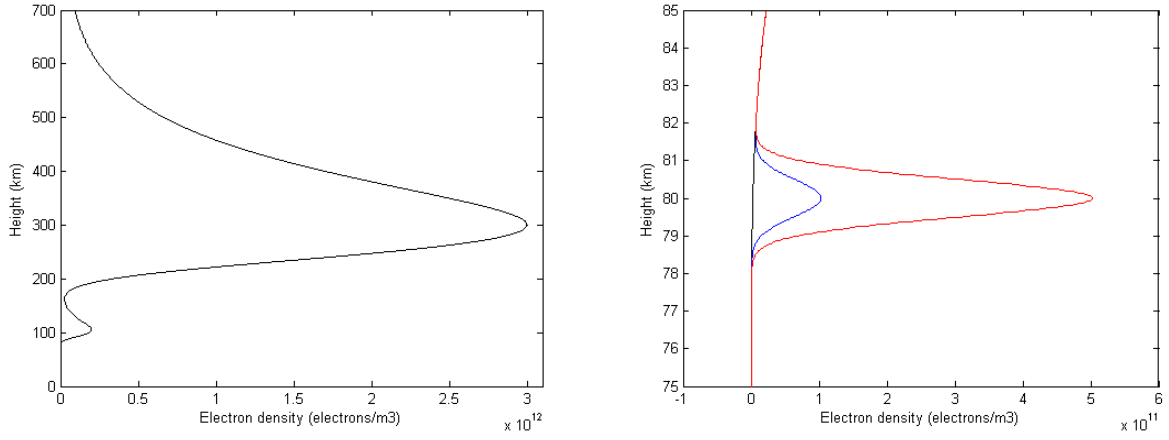

Figure 4: **Ionosphere considered in the simulations. Left plot, background electron density profile given by the Double Chapman ionosphere model, corresponding to daytime solar maximum conditions. Right plot, three different fluctuations superimposed to the background profile around 80 Km, corresponding to different ionospheric scintillation levels. Black curve: no fluctuation (B=0). Blue curve: moderate fluctuation (B=10^{11}el/m^3). Red curve: strong fluctuation (B=5 10^{11}el/m^3). X-axis: Electron density (el/m3). Y-axis: Height (Km).**

Results presented hereinafter correspond to the above described configuration. The amplitude of the simulated wave field is presented in Figure 5 and Figure 6, for the different scintillation levels, as a function of time since the start of the occultation event and RTH, respectively.

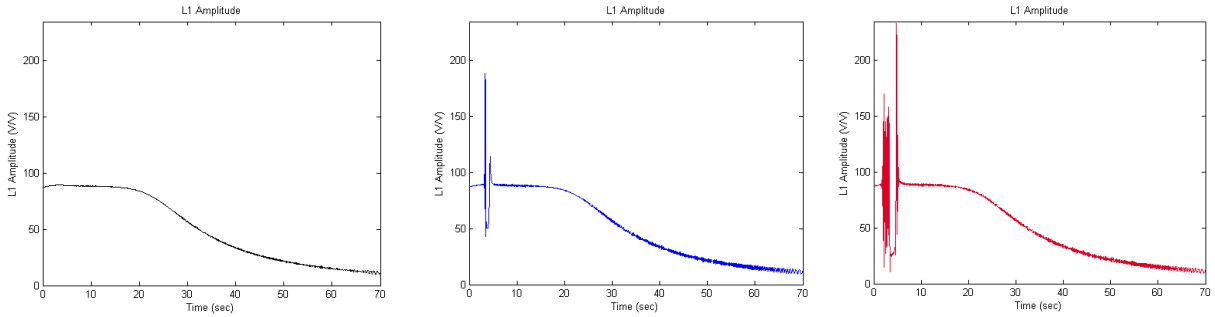

Figure 5: **Simulated amplitudes corresponding to different scintillation conditions. Left panel: no scintillation activity. Medium panel: moderate scintillation activity. Right panel: strong scintillation activity. X-axis: seconds since the start of the occultation event. Y-axis: normalized simulated amplitude at LEO (V/V).**

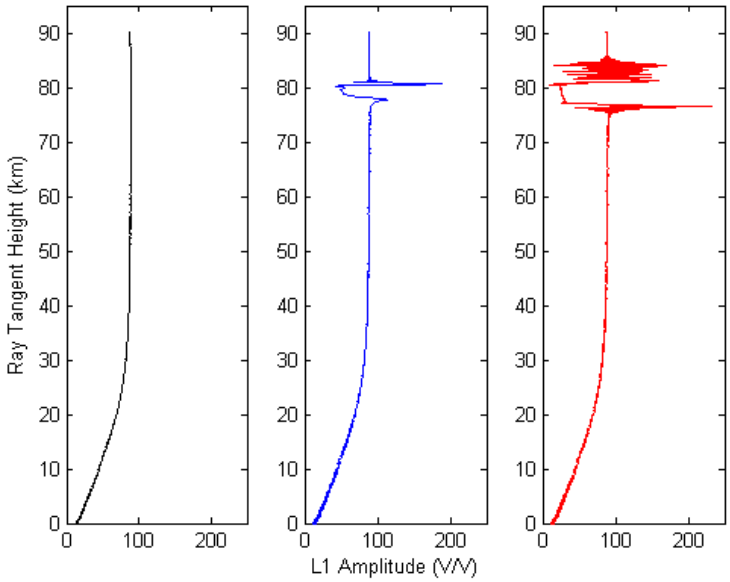

Figure 6: **Simulated amplitudes corresponding to different scintillation conditions. Left panel: no scintillation activity. Medium panel: moderate scintillation activity. Right panel: strong scintillation activity. X-axis: normalized simulated amplitude at LEO (V/V). Y-axis: Ray Tangent Height (Km).**

The peculiarity of the amplitude developed at the beginning of the occultation (between 2 and 5 seconds), shown in the middle and right panel of Figure 5, indicate scintillations due to multipath propagation. We calculated S_4 index between 40 and 90 Km of RTH for the three cases simulated and get S_4 = 0 for the no fluctuation case (left panel of Figure 5), S_4 = 0.3 for the moderate fluctuation case (middle panel in Figure 5) and S_4 = 0.6 for the strong fluctuation case (right panel in Figure 5). These values correspond to no scintillation activity, moderate activity and strong activity, respectively.

We can see how the large-scale amplitude oscillations in the middle and right panels of Figure 5 reproduce the oscillations of the electron density profile in the right panel of Figure 4. This can also be observed in Figure 6, where the amplitudes around 80 Km exhibit large oscillations, characteristic of multipath propagation.

CONCLUSIONS

This paper proposes a method for simulating ionospheric scintillation effects in RO measurements. Results show how intense electron density gradients in the E-layer produce observable scintillations at

LEO receiver, using a completely analytical model. With this method, it is possible to configure different scintillation levels, place the electron density irregularities at the desired altitude or choose the scale of the fluctuations in electron density. The flexibility of the method makes its implementation very interesting for simulating the scintillation phenomenon not only for Radio Occultations from current GNSS such as GPS, but also from future Galileo GNSS.

The mathematical formulation is adequate to describe the physical phenomenon under study. However, the different assumptions in which the method is based require a cuantitative assessment. This will be the next step of this study. A possible method could be based on reconstructing the bending agle profile from RO measurements contaminated with ionospheric scintillations, by means of wave optics inversion techniques. This bending angle could then be compared to the reference one, obtained by Abel-transforming the simulated refractivity. For future work, it will also be of importance to assess the performance of the current method with real RO data.

The model could be enhanced, for example, simulating the effect in the F-layer, or considering other electron density fluctuations. In the RO field, the method can be used to validate wave optics inversion techniques aimed at investigating the vertical structure of the ionospheric irregularities attributed to sporadic E-layers. In the satellite based navigation systems field, the model can be useful for performance assessment of algorithms for the detection of degraded ionospheric conditions. This could be an effective way to improve the robustness of GNSS against scintillation.

REFERENCES

Béniguel, Y., (2000) Characterisation of Equatorial Scintillations for Transionospheric Links. Proceedings of the 13th International Technical Meeting of the Satellite Division of The Institute of Navigation (ION GPS 2000), pp 688 – 695.

Béniguel, Y., (2002) Global Ionospheric Propagation Model (GIM): A propagation model for scintillations of transmitted signals. Radio Science, **vol. 37**, 1032, pp 13.

Fernández, L. et al, (2008) Real-Time Detection Of Ionospheric Scintillations in Galileo: Experimental Results with Real GPS Data. Proceedings of the 4th ESA NAVITEC '2008.

Forte, B. and Radicella, S. M., (2005) Comparison of ionospheric scintillation models with experimental data for satellite navigation applications. Annals of Geophysics, **vol. 48**, no. 3, pp 505-514.

Gorbunov, M. E., Gurvich, A. S. and Shmakov, A. V., (2002) Back-propagation and radio-holographic methods for investigation of sporadic ionospheric E-layers from Microlab-1 data. Int. J. Remote Sensing, **vol. 23**, no. 4, pp 675-685.

Hernández, C., et al, (2006) GALILEO Integrity: The Ground Segment Computation Algorithm Perspective. Proceedings of the 19th International Technical Meeting of the Satellite Division of The Institute of Navigation (ION GNSS 2006), pp 2634 – 2645.

Ippolito, L. J., (1999) Propagation Effects Handbook for Satellite Systems Design. Stanford Telecom, 5th Edition.

Martin, J.M., (1993) Simulation of Wave Propagation in Random Media: Theory and Applications, in Wave Propagation in Random Media (Scintillations) . Co-published by SPIE Press, Bellingham, WA, and the Institute of Physics Publishing, Bristol, UK, pp 463.

Secan, J.A., Bussey, R.M. and Fremouw, E.J., (1995) An improved model of equatorial scintillation. Radio Science, **30**, pp 607 – 617.

Sokolovskiy, S., Schreiner, W., Rocken, C. and Hunt, D., (2002) Detection of high-altitude ionospheric irregularities with GPS/MET. Geophysical Research Letters, **vol. 29**, no. 3, 1033.